

# Polarisation Characterisation in the Focal Region of a High Numerical Aperture Objective under Radial Polarisation Illumination

Hong Kang, Baohua Jia and Min Gu

Centre for Micro-Photonics, Faculty of Engineering and Industrial Sciences, Swinburne University of Technology

John Street, PO Box 218, Hawthorn, VIC, 3122, Australia

E-mail: [hkang@groupwise.swin.edu.au](mailto:hkang@groupwise.swin.edu.au)

**Abstract:** Polarisation characteristics in the focal region of a high numerical aperture objective illuminated with a radially polarised beam have been investigated with both full aperture illumination and annular illumination.

**Keywords:** radial polarisation, high numerical aperture, diffraction theory, annular.

## 1. INTRODUCTION

Nowadays, radial polarisation illumination has attracted special interest due to its unique optical properties in the focal region [1,2]. When a radially polarised beam is focused by an objective with a high numerical aperture (NA), a significant longitudinal component, which has an ultra small focal profiles, is generated in the focal region owing to the depolarisation effect [3,4]. As a result, the overall focal spot size can be greatly reduced if the longitudinal component can be enhanced. The capacity of achieving much higher resolution has thus stimulated various exciting applications with radially polarised beams including linear and nonlinear microscopy and optical laser trapping and greatly enhanced surface plasmonic wave excitation [5-10]. However, one of the most interesting properties of radially polarised beam that is the polarisation state in the focal region has been ignored in most of the research on radially polarised beam. Unlike the linearly polarised beam, in which depolarisation effect only generates strong  $E_z$  component with ignorable  $E_y$  component, in the focal region of a radially polarised beam all the three components ( $E_x$ ,  $E_y$  and  $E_z$ ) exist. This is beneficial for many applications, for example gold nanorods mediated cancer photothermal therapy [11] and optical data storage [12], in which the excitation efficiency is highly sensitive to the incident light polarisation direction. It is thus highly desirable to study polarisation characteristics of the radially polarised beam in the focal region.

In this paper, by using the vectorial-Debye diffraction theory, not only the focal field components but also the polarisation distribution of each component in the focal region of a high NA objective have been investigated. Furthermore, the manipulation of different polarisation components has been studied by employing an annular beam illumination.

## 2. CALCULATION

Fig. 1. shows a radially polarised plane wave focused by a high NA objective through an refractive-index-mismatched interface. The electric field of a radially polarised beam in the free space can be written as equation (1).

$$E = P(r)(\cos \theta \vec{i} + \sin \theta \vec{j}) \quad (1)$$

where  $P(r)$  is the amplitude position only dependent on the radial positions;  $\vec{i}$  and  $\vec{j}$  are unit vectors in the x and y directions, respectively.

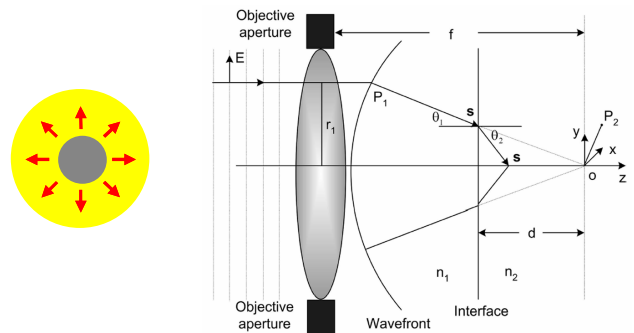


Fig. 1. Schematic focusing of a radially polarised beam.

The electric field in the focal region at point  $P_2$  can be obtained from the generalized Debye integral, expressed for a radially polarised beam as equation (2) [3].

$$E(r, \psi, z) = \frac{i}{\lambda} \int_0^\alpha \int_0^{2\pi} \sqrt{\cos(\theta_1)} \exp[-ik_0 \Phi(\theta_1)] (t_p \sin \theta_1 \cos \theta_2 \cos \varphi \vec{i} + t_p \sin \theta_1 \cos \theta_2 \sin \varphi \vec{j} + t_p \sin \theta_1 \sin \theta_2 \vec{k}) \exp[-ik_1 r \sin \theta_1 \cos(\varphi - \psi)] \exp(-ik_2 z \cos \theta_2) d\varphi d\theta_1 \quad (2)$$

where

$$\Phi(\theta_1) = -d(n_1 \cos \theta_1 - n_2 \cos \theta_2)$$

$$t_p = 2 \sin \theta_2 \cos \theta_1 / (\sin(\theta_1 + \theta_2) \cos(\theta_1 - \theta_2))$$

The indices 0, 1 and 2 denote the parameters in vacuum, medium 1 and medium 2, respectively.  $\lambda$  is the wavelength and  $k$  is the wave vector.  $\theta$  is the focusing angle between the optical axis and the propagation unit vector.  $\alpha$  is the maximal angle determined by the numerical aperture of the

objective.  $n$  is the refractive index.  $d$  is the distance from the interface to the geometric focus.  $\phi$  is the angle between the refracted electric field direction after an objective and the positive  $x$  axis.  $\psi$  is the angle between the electric field direction in the focal plane and the positive  $x$  axis. In our calculation, we assume the focal plane the same as the  $x$ - $y$  plane ( $d=0$ ). A plane wave and a water immersion aplanatic objective of NA 1.2 are used.  $n_1$  and  $n_2$  are 1.515 and 1.33, respectively. The illumination wavelength is 780 nm. Equation (2) shows that the diffraction field in the focal region of a high NA objective has three components in the  $x$ ,  $y$  and  $z$  directions.

In Fig. 2, the strength of different field components along the  $x$  axis in the focal plane is presented. It is clearly seen that all three components exist in the focal region and the maximal intensity of the longitudinal component is nearly three times that of the transverse component. Due to the dominant strength of the longitudinal components, the overall focal spot size is much narrower compared to the size of the transverse component.

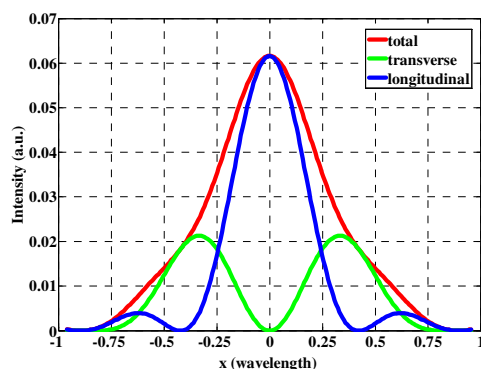


Fig. 2. Intensity profiles in the focus under radial illumination with NA 1.2.

Fig. 3 shows the electric field vectors in the focal region under radial polarisation and linear polarisation projected on the  $x$ - $y$  plane demonstrating a radially polarised beam is capable to produce a more uniform electric field distribution.

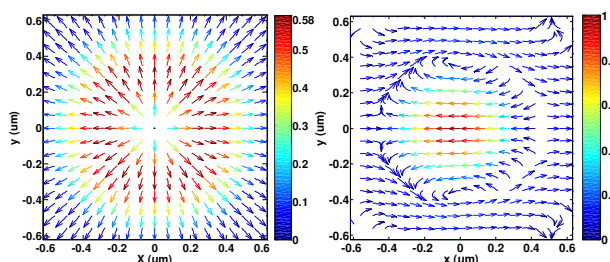


Fig. 3. Electric field vectors of a radially polarised beam (left) and a linearly polarised beam (right) projected on the  $x$ - $y$  plane with an objective of NA 1.2 ( $z=0$ ).

In order to manipulate the weighting of the electromagnetic field in the  $x$ ,  $y$  and  $z$  directions, a circular opaque disk can be used to block the central part of the beam, in which situation only the beam with large converging angles makes contribution to the optical properties in the focus. Therefore, the longitudinal component contributes more to the focus, resulting in the larger electric field magnitude ratio at peaks between longitudinal component and transverse one as the radius of the opaque disk increases. For example, when the epsilon defined as the radius ratio of the opaque disk and the

objective's back aperture is equal to 0 and 0.7, the ratio at peaks between longitudinal component and transverse one is 2.89 and 5.03, respectively.

### 3. SUMMARY

We have investigated the polarisation characteristics of a radially polarised beam in the focal region of a high NA objective. A more uniform electric field distribution in the focal region under radial polarisation can be generated compared with linearly polarised beam. By employing a circular opaque disk, the ratio of the longitudinal component and the transverse one can be manipulated, which could be beneficial for applications including laser trapping and photothermal therapy.

Acknowledgement: The authors thank the Australian Research Council for its support.

### REFERENCES

- [1] S.Sato, Y. Harada and Y. Waseda, "Optical trapping of microscopic metal particles", *Opt. Lett.* vol. 19, pp. 1807-1809, 1994.
- [2] V. G. Niziev and A. V. Nesterov, "Influence of beam polarization on laser cutting efficiency," *J. Phys. D.* vol. 32, pp. 1455-1461, 1999.
- [3] Min Gu, *Advanced Optical Imaging Theory*, Springer, 2000.
- [4] Baohua Jia, Xiaosong Gan, and Min Gu, "Direct measurement of a radially polarized focused evanescent field facilitated by a single LCD," *Opt. Express*, vol. 13, pp. 6821-6827, 2005.
- [5] E.Y.S. Yew and C.J.R. Sheppard, "Second harmonic generation polarization microscopy with tightly focused linearly and radially polarized beams," *Opt. Commun.* vol. 275, pp. 453-457, 2007.
- [6] Y. Kozawa and S. Sato, "Observation of the longitudinal field of a focused laser beam by second-harmonic generation," *J. Opt. Soc. Am. B: Opt. Phys.* vol. 25, pp. 175-179, 2008.
- [7] K.J. Moh, X.C. Yuan, J. Bu, S.W. Zhu, and B.Z. Gao, "Surface plasmon resonance imaging of cell-substrate contacts with radially polarized beams," *Opt. Express*, vol. 16, pp. 20734-20741, 2008.
- [8] T.A. Nieminen, N.R. Heckenberg, and H. Rubinsztein-Dunlop, "Forces in optical tweezers with radially and azimuthally polarized trapping beams," *Opt. Lett.* vol. 33, pp. 122-124, 2008.
- [9] H. Wang, L. Shi, B. Lukyanchuk, C. Sheppard, and C.T. Chong, "Creation of a needle of longitudinally polarized light in vacuum using binary optics," *Nature Photonics*. vol. 2, pp. 501-505, 2008.
- [10] N.M. Mojarad and M. Agio, "Tailoring the excitation of localized surface plasmon-polariton resonances by focusing radially-polarized beams," *Opt. Express*, vol. 17, pp. 117-122, 2009.
- [11] Jingliang Li, Daniel Day and Min Gu, "Ultra-low energy threshold for cancer photothermal therapy using transferrin-conjugated gold nanorods," *Adv. Mater.* vol. 20, pp. 3866-3871, 2008.
- [12] Xiangping Li, James W. M. Chon, Shuhui Wu, Richard A. Evans, and Min Gu, "Rewritable polarization-encoded multilayer data storage in a 2,5-dimethyl-4-(p-nitrophenylazo)anisole doped polymer," *Opt. Lett.* vol. 32 (3), pp. 277-279, 2007.